OPTICAL FIBER BASED LOSS MONITOR FOR ELECTRON STORAGE RING

T. Obina#, Y. Yano, KEK, Tsukuba, Ibaraki 305-0801, Japan

Abstract

A beam loss monitor using optical fibers has been developed to determine the turn-by-turn loss point of an injected beam at the Photon Factory (PF) 2.5-GeV electron storage ring. Large-core optical fibers were installed along the vacuum chamber of the storage ring that can cover the entire storage ring continuously. There are many kinds of beam loss monitors for high energy accelerators, such as PIN diode detector, ionization chamber using coaxial cable, Cherenkov light detector, etc. Among these methods, optical fibers are suitable to determine the beam loss point because of the ease of covering the entire ring with them, they have better time and position resolution, and they are cost effective. In this report, review of beam loss monitors for electron storage rings and LINACs are reported at first, then the result of the optical-fiber beam loss monitor at the KEK-PF are reported. Long-term deterioration by radiation is also reported.

INTRODUCTION

Overview of Loss Detection

Beam loss detections are one of the most important instruments to operate particle accelerators. It can be classified according to the purpose of the system, namely, personnel protection system (PPS) and machine protection system (MPS). The PPS requires absolute radiation level monitor to ensure the personnel safety and its typical time range is from seconds to minutes order, and typical MPS is used in faster time range from seconds down to micro seconds. The importance of MPS depends on the beam power of the accelerator. Reliable and fast MPS are mandatory tool at high power proton machine such as LHC, J-Parc and SNS, high beam current electron machine such as KEK B-Factory or PEP-II, and high-average DC machine such as ERL or ELBE.

On the other hand, beam loss monitors are not only instruments for PPS and MPS but also quite useful for advanced beam diagnostics. With the aid of fast loss monitors, machine commissioning becomes easy and further machine tuning can be realized with such loss monitors. In this paper, basic principle of loss monitor that is common for PPS, MPS and tunings are described shortly, and the principle of optical fiber loss monitor which can be useful for machine tuning are described in detail.

There are many good reference papers and textbooks have been published already. As a reference to general overview and implementation, CERN Accelerator School (CAS) 2008 by K. Wittenburg [1] and an invited talk at Beam Instrumentation Workshop (BIW) 2010 by A. Zhukov [2] and their referenced papers are nice summary to start. In case you have more interest on beam collimation and machine protection, CAS 2011 textbook by R. Schmidt [3] are good point to start.

#takashi.obina@kek.jp

Motion of Lost Electrons and Simulation Codes

When an electron passes through some kinds of medium, it interacts with the medium depending on its energy. Mathematical representations are well described in the review of particle physics data group [4,5]. Stopping-power and range tables for electrons are available on the web site by NIST [6].

Interactions between photons and medium are also well represented in many papers. X-ray form factor, attenuation and scattering tables are referenced at the web site of NIST [7,8].

Wide varieties of simulation codes are available in these days. There are so called “five major codes”, MCNPX, FLUKA, MARS, PHITS and GEANT4. These codes have different characteristics and a comparison of these codes is available on the web [9]. In this paper, we used EGS5 code [10] which can simulate electron gamma shower developed by SLAC and KEK. Figure 1 show an example of electron trajectory when a stray electron hits the vacuum chamber wall. It is clear that the effective thickness of the chamber is much longer than real thickness, and produces many secondary particles. We can detect many secondary electrons where the thickness is much thin such as bellows.

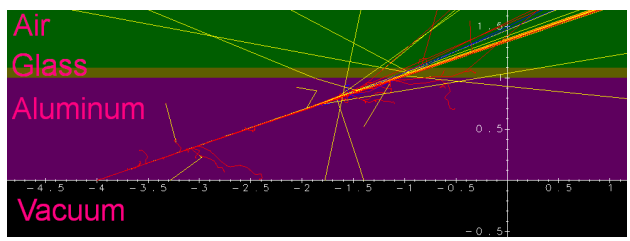

Figure 1: Simulation example of EGS5. Trajectory of a 2.5 GeV electron into 1 cm thickness Aluminum vacuum chamber. Red, blue and yellow line represents electron, positron and photon, respectively.

History of Loss Monitor Using Optical Fibers

Usually we can put beam loss monitors at the outside of the vacuum chamber. In the electron storage ring or injector linac, widely-used loss monitors are scintillation counter, PIN diode, Ionization chamber, Optical fiber, etc. The optical fiber based loss monitors are described in detail in this paper. Please refer to refs [1-3] for other type of loss monitors.

ISBN 978-3-95450-127-4

Before 1990s, optical fiber is mainly used as light guide of scintillation detector or scintillator. As reported in ref [11], Pishchulin suggested to use optical fiber as beam current monitor. In 1995, P. Gorodetzky and R. DeSalvo et.al. reported papers about the calorimetry with quarts fiber [12-14] for LHC detector. They performed many calculation, simulation and experiments using Cherenkov radiation produced in optical fibers.

From 1990, at the Tesla Test Facility 1 (TTF1), 100-m length Germanium- and Phosphorus-doped fiber was used as dosimeters [15]. It is possible to detect the loss point by using optical time domain reflectometry (OTDR). In order to detect the loss point with high position resolution, Cherenkov light in the fiber is also used at TTF1 [16, 17] and in successive experiments at FLASH [18, 19].

Many accelerator laboratories used optical fiber as loss monitor. For example, T. Kawakubo already reported the fast response loss monitor using fiber in 2000 [20, 21]. At DELTA [22] and Metrology Light Source [23] adopted same system as DESY. Fiber loss monitor at Advanced Photon Source (APS) is reported in ref. [24]. At SPring-8, SCSS and SACLA, fiber loss monitor has been intensively developed and has been used as very effective tool for commissioning and beam tuning [25-28]. At ALICE in Daresbury developed a spliced fiber for loss detection [29]. Recently, in 2012, J. W. van Hoorne developed fiber loss monitor for CLIC, and summarized as his master thesis [30]. Note that this is not a complete list of fiber loss monitor for accelerators.

Cherenkov Radiation in Optical Fiber

A Cherenkov radiation is produced when a charged particle passes through a medium at a speed greater than the phase velocity of light in that medium. In case of glass with the refraction index n is equal to 1.6, threshold speed is $0.625v_c$ where v_c the speed of light in vacuum, and the Cherenkov angle $\cos\theta_c = 1/\beta n$ is equal to 52 degree. Number of photons per unit length per unit energy interval N is expressed using wavelength as [5]

$$\frac{d^2N}{dxd\lambda} = \frac{2\pi\alpha}{\lambda^2}\left(1 - \frac{1}{n^2}\right)$$

where α is file structure constant. By using photo multiplier tube (PMT) with its effective wavelength range from 300 to 600 nm [31], we can get enough photons.

PRINCIPLES OF LOSS DETECTION

Electrons that are not captured in the storage ring hit the vacuum chamber wall and produce secondary electrons outside the vacuum chamber. Secondary electrons that run through quartz fiber generate Cherenkov light provided the energy of the electrons is high enough. As shown in Fig. 2, a photomultiplier tube (PMT) is used for the detection of a light pulse. There are three candidates for the PMT layout: one PMT at the upstream end, one PMT at the downstream end, and a PMT at both ends of the fiber. We adopted to use one PMT on the upstream side because of its better time

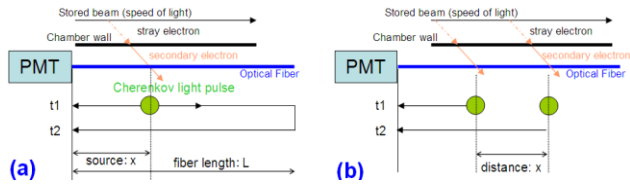

Figure 2: Schematic drawing of detection principle for: one loss point (a), and two loss points (b). In both cases, the loss is coming from a single bunch.

resolution than the downstream end, and the small reflection produced by the opposite side of a fiber can determine the exact location of the light pulse.

With one loss point, as shown in Fig. 2(a), the source position is determined by measuring the arrival time of the direct light (t_1 in the figure) and the reflected light (t_2), using simple arithmetic $x=L-(t_2-t_1)*v_{fiber}/2$, where v_{fiber} is the speed of light propagation in a glass medium, which is equal to $^2/_3$ the speed of light in a vacuum (v_c).

Figure 2(b) shows a case where two light pulses are produced by a single passage of a bunch. The time difference between two direct pulses becomes longer because the direction of the electron bunch and the light pulse are opposite. It is useful to introduce an "effective" propagation time for the calculation of two direct pulses: $v_{eff} = 2/5 * v_c$ (equivalent to 8.3 ns/m).

The beam loss timing and Cherenkov light propagation is also described in step-by-step slides in the presentation file of this talk.

Determination of Loss Location

Figure 3 shows an example of PMT output measured in the PF-Ring during injection. Details of measurement setup are shown in later section. We can observe large peaks marked as B, C, and D in the figure and small peaks at E and F. In order to determine which pulses are coming from a direct path or a reflected path, we attached a reflector on the downstream end of the fiber.

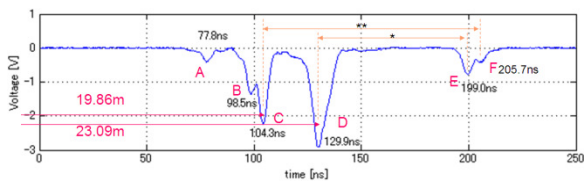

Figure 3: Example of loss signal during injection. These peaks disappear when we stop electron beam injection.

Figure 4 shows an example with and without a reflector. In this way, we determined that peaks E and F in Fig. 3 are reflections from the downstream end. Next, by assuming peak E to be a reflection from D and by applying the method in Fig. 2(a), the distance from the PMT to peak D is estimated to be 23.08 m. In the same way, the distance of peak C is estimated to be 19.86 m from the PMT by assuming peaks C and F are a pair. We can conclude that the distance between peaks C and D is 3.23 m from the reflection signal.

ISBN 978-3-95450-127-4

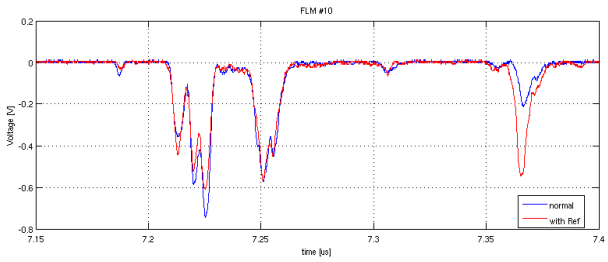

Figure 4: Signal without (blue) and with (red) reflector.

To cross-check this measurement, it is important to utilize the time difference of peaks C and D. By applying the procedure in Fig. 2(b), the distance between C and D is estimated to be 3.1 m, which shows good agreement with 3.23 m. On the downstream-end of the fiber, peaks B and C are squeezed and only one peak—F—is observed.

LOSS MONITOR AT KEK-PF

As a summary talk of the conference, following sections include similar description in the previous work [32] except for the effect of radiation deterioration in two years of operation.

The KEK Photon Factory (PF) is 2.5-GeV electron storage ring for dedicated synchrotron radiation source. An electron bunch is injected directly from a linear accelerator that is shared by KEKB-HER, -LER and PF-AR [33]. The three rings (PF, KEKB-HER, -LER) share the linac pulse-by-pulse at a maximum rate of 50 Hz. Because ambient temperature affects the stability of a large water cooling plant, we sometimes need to adjust the injection parameters—such as injection energy or injection angle to the storage ring. A beam loss monitor which can cover whole ring with high position and time resolution is strongly desired for this kind of tuning procedure.

Optical fibers are suitable for our purpose because of the ease of covering the entire ring with them, they have better time and position resolution than other methods such as PIN diode or ionization chamber, and they are cost effective. On the other hand, they have disadvantages, such as needing an external trigger, their difficulty in detecting CW loss, they provide small coverage in the plane perpendicular to the beam, and there is difficulty in the calibration of absolute beam loss.

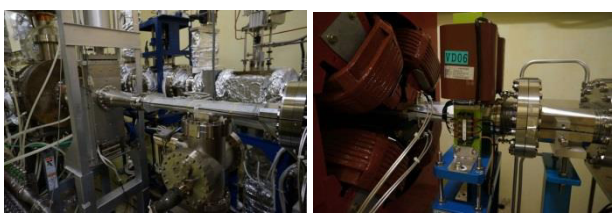

Figure 5: Black cables mounted on the side of the vacuum chamber are the optical fibers for the loss monitor. The fibers can be fed through the magnet due to the non-magnetic nature of the medium.

MEASUREMENT SETUP

In this study, first we tested the fiber beam loss monitor in a location where the normalized horizontal aperture is small, and then we installed a total 10 fibers to cover the circumference of the entire ring circumference.

We selected 600-μm core, all-silica, low-OH, step-index large-core optical fibers, manufactured by OFS Furukawa (parts number:CF01493-14) [34]. They were installed along the inner wall of the vacuum chamber to cover the entire storage ring continuously. Figure 5 shows an example of installation. The fibers can be fed through between magnet and vacuum chamber due to the non-magnetic nature of the medium. In total, 10 optical fibers with a length of 30 m were used. Both ends of the fibers are fed out through the radiation shield of the ring, and a photomultiplier tube (H10721-110, Hamamatsu Photonics [31], with spectral response from 230 to 700 nm, gain from 10^4 to 10^6) is attached to the upstream side of the fibers. The sensitivity of the PMT is sufficiently high to detect loss at the PF-Ring, and its short rise-time of about 0.57 ns is fast enough to determine the location of the beam loss point. The PMT has a built-in high-voltage power supply. A standard oscilloscope (Rohde&Schwarz RTO1024) together with the external injection trigger was used for the measurements.

In order to reduce the number of PMTs and fibers, the PMTs can be sited on the inside of the radiation shield wall or optical fiber cables longer than 50 or 100 m can be used. The disadvantages of such an approach includes the fact that identification of the beam loss point becomes slightly more complicated, connecting or removing PMTs during machine operation is not possible, and the attenuation of the light pulse becomes larger. We are reviewing the optimal number and length of fibers, before putting optical fibers on the outside, top and bottom of the vacuum chamber.

RESULTS

Figure 6 shows the results for turn-by-turn loss detection of an injected beam. Note that the vertical axis is auto-scaled, and not every turn is plotted. On the first turn, the beam is lost upstream of undulator U#02 indicated as 1 and 2 in red in the figure. On the second turn or fourth turn, a large loss is detected downstream of the pulsed sextupole magnet (PSM). Large losses are observed on the 2nd , 4th , 7th turns because the horizontal tune is equal to 9.60 in the KEK-PF. Taking into account the injection angle and normalized apertures of the storage ring, the result agrees with the simulation.

Triggering the septum and kicker magnets without an injection beam does not show any peak in the PMT output, and we confirmed the beam loss shown in Fig. 6 is not coming from stored beam. The signal-to-noise ratio is good enough to distinguish the loss from the stored beam or other PMT noise from the beam loss signal only from the injected beam.

ISBN 978-3-95450-127-4

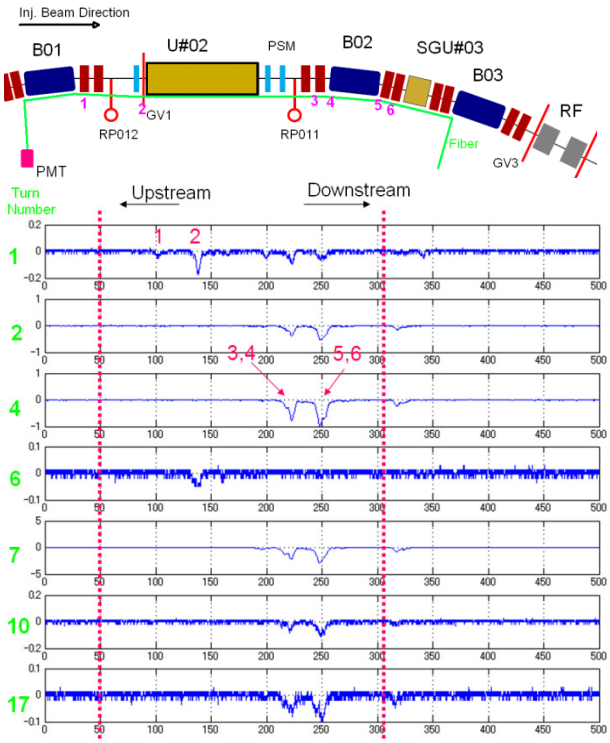

Figure 6: Layout of storage ring components and optical fibers (top) and detected loss signal (bottom) on each turn. The electron beam travels from left to right in the figure.

The peaks in the figure appear in locations where the fibers are attached to bellows or the thickness of the chamber wall is thinner than in other locations.

Position resolution depends on the rise time of the PMT and the length of the fibers and cables between the PMT and oscilloscope. From the output signal, we can distinguish two peaks at 2-3 ns apart, which correspond to a position resolution of about 30 cm. The resolution is good enough compared with the distance between accelerator components.

Beam Losses of Entire Ring Circumference

Figure 7 shows beam loss for the entire ring. We used the same PMT with the same gain to measure all 10 fibers to ensure the output voltage of the PMT is equal to the same beam loss. Of course this is not an accurate measurement because the detected losses depend on the thickness of the walls of the vacuum chamber, however, it is still useful for an estimation of beam loss around the ring. The beam loss shown in Fig. 7 is the summary of 10 injections. The peak voltage of each signal depends on the charge, energy spread and position of the injected beam. We confirmed the output voltage and the loss location are sometimes different pulse-to-pulse, but show almost a similar loss pattern. Figure 7 shows a typical pattern during kicker injection.

In the KEK-PF, the horizontal normalized aperture is small at three locations: septum magnet, vertical wiggler,

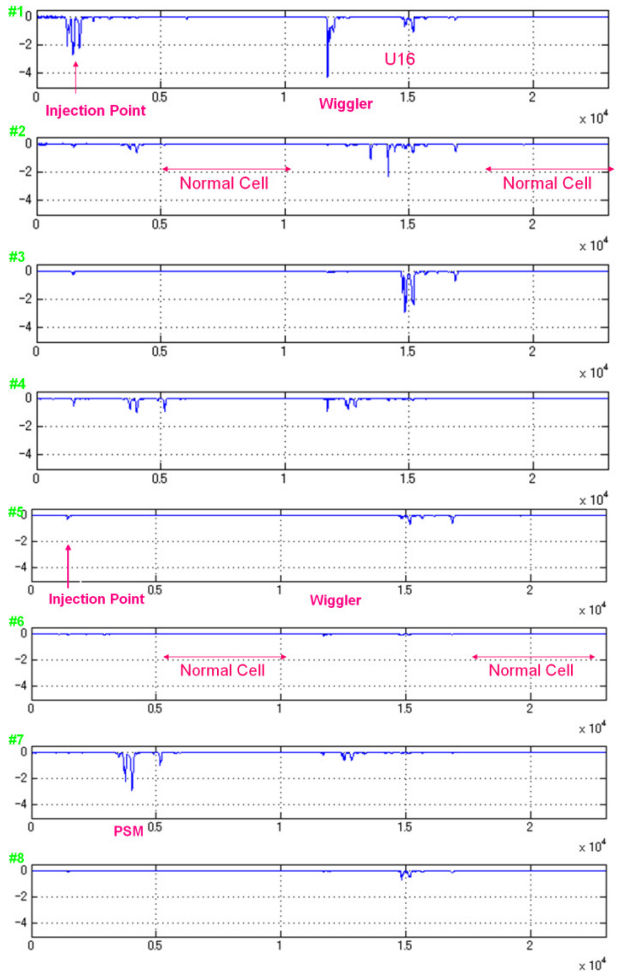

Figure 7: Beam loss over the whole ring. In each row, the horizontal full scale corresponds to the entire ring circumference of 187 m.

and pulsed sextuple magnet. These locations show a large loss, as expected. The aperture is large at a normal cell, and there is almost no loss there.

Kicker and PSM Injection

Two injection systems have been used for routine operation: kicker magnets and a PSM [35]. Schematic diagram of two injection system are shown in Fig. 8. The

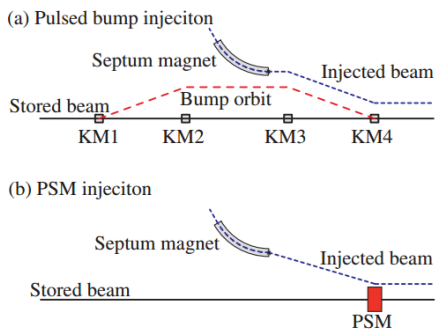

Figure 8: Schematic diagram of kicker injection and pulsed sextupole injection.

ISBN 978-3-95450-127-4

fiber loss monitor is useful for analyzing the turn-by-turn difference of the beam loss pattern. Figure 9 shows an example of PMT voltage with the two injection methods measured downstream of the vertical wiggler. Kicker injection shows a large loss at the first turn and fourth turn, whereas PSM injection shows no loss of beam at the first turn, but a large loss at the second turn. The pulsed sextupole magnet deforms distribution in the phase space of the injected beam, so the loss point is different from kicker injection. Detailed analysis and optimization of injection parameter for PSM injection are under way.

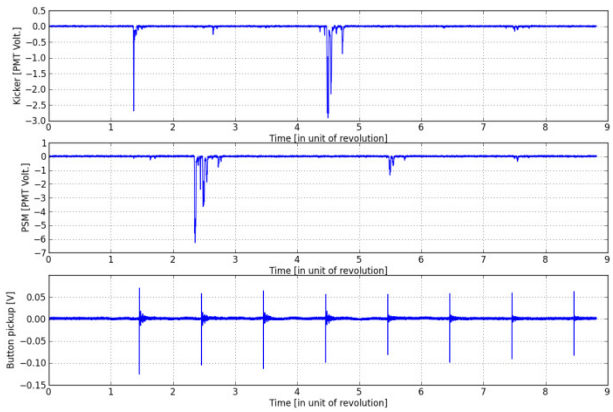

Figure 9: Beam loss measured using two injection systems: kicker magnets (top) and a pulsed sextupole magnet (middle). The bottom figure shows the signal from a button pickup electrode near the vertical wiggler. No beam is stored in the ring prior to injection. The horizontal axis represents the turn number, namely, time in unit of revolution of the PF-Ring

DETERIORATION BY RADIATION

The optical fibers have been mounted on the vacuum chamber for about two year after installation. Total operational time of the PF-Ring is about 18 months during this period. We measured the transmission factor of the optical fibers and found that there was no significant deterioration after the 18 months of operation. Some fiber showed a 10 % decrease in transmission factor, but that was located in the normal cell where there is no loss during injection. The factor of 10 % has almost no effect on loss measurement. There remains ambiguity in the transmission factor measurement. Because we did not have a good light source in the range of PMT, we measured the transmission using a wavelength of 850 nm. This is different from the PMT range and is not the wavelength of Cherenkov light. We plan to prepare a light source of PMT range.

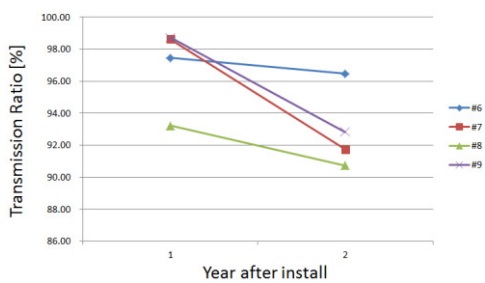

Figure 10: Transmission ratio of optical fiber and its change after installation.

SUMMARY AND FUTURE PLAN

A beam loss monitor using optical fibers was developed to determine the loss point of an injected beam at the PF-Ring. The time resolution was good enough to distinguish a distance of about 30 cm along the vacuum chamber, and turn-by-turn measurement was achieved.

Development of a real-time display system that can cover the entire ring with every injection bunch is under way. This will become an indispensable tool for the tuning of the linac, beam transport line and injection parameters. The same beam loss detection system has been used for the compact ERL (cERL) in KEK, where beam loss detection is a key issue for operation. During the commissioning of cERL, we measured beam loss with the beam energy about 5 MeV. We plan to use the optical fiber loss monitor for the Super-KEKB.

REFERENCES

[1] K. Wittenburg, CERN Accelerator School (CAS) 2008, “Beam Loss Monitors”, CERN-2009-005 (2009) 249
[2] A. Zhukov, “Beam Loss Monitors (BLMs): Physics, Simulations and Applications In Accelerators”, Proc. BIW10, Santa Fe, New Mexco (2010) 553
[3] R. Schmidt, CAS 2011, “Machine Protection and Collimation”
[4] J. Beringer et al. (Particle Data Group), “ Review of Particle Physics” Phys. Rev. D 86, 010001 (2012), 30. PASSAGE OF PARTICLES THROUGH MATTER
[5] Particle Data Group, http://pdg.lbl.gov/
[6] Electron stopping-power and range tables, http://physics.nist.gov/PhysRefData/Star/Text/ESTAR.html
[7] C.T. Chantler et al, "Detailed Tabulation of Atomic Form Factors, Photoelectric Absorption and Scattering Cross Section, and Mass Attenuation Coefficients for Z = 1-92 from E = 1-10 eV to E =0.4-1.0 MeV", NIST, http://www.nist.gov/pml/data/ffast/index.cfm
[8] J. H. Hubbell, et al. “Pair, Triplet, and Total Atomic Cross Sections (and Mass Attenuation Coefficients) for 1 MeV-100 GeV Photons in Elements Z=1 to 100” , NIST, http://www.nist.gov/data/PDFfiles/jpcrd169.pdf
[9] “Code Comparison Chart for All-Particle Monte Carlo Codes”, http://mcnpx.lanl.gov/opendocs/misc/chart.ppt
[10] EGS5 homepage, http://rcwww.kek.jp/research/egs/
[11] I. Pishchulin et al. “Optical fiber Cherenkov detector for beam current monitoring”, PAC91 (1991) 1567
[12] R. DeSalvo, et al., “Recent developments in quartz fibre calorimetry”, Nucl. Instr. and Meth. A 357 (1995) 369
[13] R. DeSalvo, et al., “Quart fibre calorimetry – Monte Carlo simulation”, Nucl. Instr. and Meth. A 357 (1995) 380
[14] P. Gorodetzky et al., “Quarts fibre calorimetry” Nucl. Instr. and Meth. A 361 (1995) 161

ISBN 978-3-95450-127-4

[15] H. Henschel et al., “Fiber Optic Radiation Sensing Systems for TELSA” TESLA-Report No. 2000-25, 2000
[16] E. Janata, “Determination of location and intensity of radiation through detection of Cherenkov emission”, Nucl. Instr. and Meth. A 493 (2002) 1
[17] E. Janata, et al., "Determination of location and intensity of radiation through detection of Cherenkov emission in optical fibers. Part 2. preliminary results obtained at TTF", Nucl. Instr. and Meth. A 523 (2004) 256
[18] M. Körfer et al., “Fiber optic radiation sensor systems for particle accelerators” NIM A526 (2004) 537
[19] F. Wulf and M. Körfer, “Local Beam Loss and Beam Profile Monitoring with Optical Fibers”, Proc. DIPAC09 (2009) 411
[20] T. Kawakubo et al., “Fast-response beam loss monitor”, Proc. ICANS-XV, 2000.
[21] T. Kawakubo et al., “High speed beam loss monitor and its deterioration by radiation”, Proc. EPAC04 (2004) 2652
[22] G. Schmidt, et al., “Optical Fibre Beam Loss Monitors for Storage Rings at DELTA”, Proc. EPAC02 (2002) 1969
[23] J. Bahrdt, et al. “Cherenkov Fibers for Beam Diagnostics at the Metrology Light Source”, Proc. PAC09 (2009) 1159
[24] J. C. Doolingy, et al. “Development of a Fiber-Optic Beam Loss Position Monitor for the Advanced Photon Source Storage Ring”, Proc. PAC09 (2009) 3438
[25] X.-M. Maréchal, et al., “Beam Based Development of a Fiber Beam Loss Monitor for the Spring-8/XFEL,” DIPAC09, Basel, Switzerland (2009) 234.
[26] Y. Asano, et al., “First Operation of a Fiber Beam Loss Monitor at the SACLA FEL”, Proc. IPAC2011, San Sebastián, Spain (2011) 2367.
[27] T. Itoga, et al., “Availability of Fiber Based Beam Loss Monitor at SACLA XFEL Facility,” ERL2011 Tsukuba, Japan (2011) WG4.
[28] X.-M. Maréchal, et al., “Design, development, and operation of a fiber-based Cherenkov beam loss monitor at the Spring-8 Angstrom Compact Free Electron Laser”, Nucl. Instr. and Meth. A 673 (2012) 32
[29] A. Intermite, et al., “Cherenkov Fibre Optic Beam Loss Monitor at ALICE”, Proc. IPAC2011 (2011) 1383
[30] J. W. van Hoorne, “Cherenkov Fibers for Beam Loss Monitoring at the CLIC Two Beam Module”, Master thesis, Jun 2012, http://cds.cern.ch/record/1476746
[31] Hamamatsu Photonics, http://www.hamamatsu.com/
[32] T. Obina, Y. Yano, “Optical-Fiber Beam Loss Monitor for the KEK Photon Factory”, Proc. IBIC12 (2012) 351
[33] K. Tsuchiya, et al., “Present Status of the KEK PF-Ring and PF-AR”, IPAC13, Shanghai, China (2013) 136
[34] OFS Furukawa, http://www.specialtyphotonics.com/
[35] H. Takaki et al. “Beam injection with a pulsed sextupole magnet in an electron storage ring”, Phys. Rev. ST Accel. Beams 13, 020705 (2010)

ISBN 978-3-95450-127-4